Bioorganic Chemistry 104 (2020) 104214

Contents lists available at ScienceDirect

Bioorganic Chemistry

journal homepage: www.elsevier.com/locate/bioorg

Activity and specificity studies of the new thermostable esterase EstDZ2

Kamela Myrtollari[a], Nikolaos Katsoulakis[a], Dimitra Zarafeta[b], Ioannis V. Pavlidis[a], Georgios Skretas[b], Ioulia Smonou[a,*]

[a] Department of Chemistry, University of Crete, University Campus-Voutes, 70013 Heraklion, Crete, Greece
[b] Institute of Chemical Biology, National Hellenic Research Foundation, 11635 Athens, Greece

ARTICLE INFO

Keywords:
Thermostable esterase
Hydrolysis
Kinetic resolution
In-silico analysis

ABSTRACT

In this paper, we study the activity and specificity of EstDZ2, a new thermostable carboxyl esterase of unknown function, which was isolated from a metagenome library from a Russian hot spring. The biocatalytic reaction employing EstDZ2 proved to be an efficient method for the hydrolysis of aryl *p*-, *o*- or *m*-substituted esters of butyric acid and esters of secondary alcohols. Docking studies revealed structural features of the enzyme that led to activity differences among the different substrates.

1. Introduction

Lipolytic enzymes (EC 3.1.1.x) catalyze the hydrolysis of carboxyl ester bonds and they can be further grouped into several subclasses based on their substrate specificity and their capacity to hydrolyze esters in solution and emulsion. EC 3.1.1.1 represents carboxylesterases, enzymes which are active on solutions of short acyl chain esters [1]. The second more widely used subclass includes lipases, which are represented as EC 3.1.1.3 enzymes [2]. It is generally established that lipases have the unique capacity to cleave carboxylic ester bonds of water-insoluble long chain triacylglycerols including natural fats. Moreover, lipases, unlike esterases, are interfacially activated [3].

However, this classical distinction between lipases and esterases should no longer be considered as the main distinction between these hydrolytic enzymes, as kinetic and structural studies have revealed that there are lipases that can hydrolyze water-insoluble-long-chain esters without bearing a lid domain [4]. Therefore, the distinction between esterases and lipases should no longer be correlated with the physical state of the substrate and/or the presence of a lid domain in the enzyme molecule [5].

Lipolytic enzymes constitute one of the most abundant class of enzymes and they have received great attention as they participate in a variety of biological processes due to their functional diversity [6]. Their functions are pivotal for the human body via digestion, as they provide building blocks for biosynthesis, help the detoxification and provide carbon sources for energy [7]. In addition to their fundamental biological importance, lipolytic enzymes have many potential industrial and medicinal applications. Increasing interest revolves around their potential applications in the pulp- and paper-making industries [8]. Besides their ability to catalyze hydrolysis, lipolytic enzymes can also catalyze synthesis of ester bonds or transesterification reactions in non-aqueous media, following the thermodynamic reversion of the hydrolysis reaction route [9]. All these features render them protagonist biocatalysts in the industry [10].

Their biotechnological significance is reflected by the fact that there is an enormous effort to find techniques and methods, which will allow exploration of microbial organisms residing in extreme environments [11]. Metagenomics is one of the approaches, which aims to address this issue and bypass the limitations imposed by current culturing techniques [12]. Such recently developed techniques have provided access to new esterases or lipases bearing novel sequences and important features, such as thermostability, which is a crucial prerequisite for industrial applications.

EstDZ2 is a new lipolytic enzyme, which we have recently isolated from a metagenomic sample from a hot spring located in the Kamchatka Peninsula (Russia) as a part of the international project Hotzyme, which aims at identifying novel thermostable hydrolytic enzymes derived from hot springs with properties suitable for industrial applications [13]. The isolated esterase, was cloned, purified from *Escherichia coli* and characterized biochemically [14]. According to activity and specificity studies EstDZ2 can efficiently catalyze the hydrolysis of short to medium-length acyl chains esters [15]. The biochemical characterization proved that this new esterase is a thermostable enzyme with a half-life of more than six hours and excellent stability at high concentrations of organic solvents [15]. These properties suggest that EstDZ2 could be utilized in many different industrial applications. Furthermore, EstDZ2 is an interesting enzyme from a phylogenetic point of view, since its amino acid sequence did not cluster with that of any previously

* Corresponding author at: Department of Chemistry, University of Crete, 70013, Heraklion, Crete, Greece.
E-mail address: smonou@uoc.gr (I. Smonou).

https://doi.org/10.1016/j.bioorg.2020.104214
Received 28 February 2020; Received in revised form 23 July 2020; Accepted 30 July 2020
Available online 29 August 2020

characterized bacterial esterolytic enzyme and, thus, it was found to belong to a putative new family of bacterial esterolytic enzymes, for which we have proposed the index XV [15].

In this work, we have examined in more detail the biochemical profile of the new thermostable esterase EstDZ2 by studying its reactivity and specificity towards aryl *p*-substituted esters of butyric acid and esters of secondary alcohols, and have found that EstDZ2 can successfully hydrolyze a wide range of esters. *In silico* analysis reveals that the activity of this new enzyme is a function of the geometry of the active site and the structure of the bulky substrate. These are the first reported reactions catalyzed by EstDZ2 and may eventually lead to utilization of this enzyme as a potent catalyst in organic synthesis.

2. Results and discussion

Recently published detailed biochemical characterization of EstDZ2 revealed that the three-dimensional modelled structure of the new hydrolytic enzyme is characterized by the α/β hydrolase fold, forming a twisted β-sheet [15]. The catalytic triad is constituted by residues of Ser, Asp and His, which are typical for esterolytic enzymes. Due to its novel sequence and functional characteristics, EstDZ2 is classified to a new family of bacterial esterolytic enzymes [15]. To investigate its esterolytic activity and optimize reaction conditions, *p*-nitrophenyl butyrate was used as a substrate since it is a pH-indicator and there is significant literature for *p*-nitrophenyl butyrate resolutions catalyzed by hydrolases [16–18]. The reaction conditions were optimized after measurements of EstDZ2 activity in a wide range of pH and temperatures, where it was found that EstDZ2 exhibits its maximal activity at 50 °C and pH 8.0 as also reported previously [15].

Initial screening of the new esterase with different *p*-nitrophenyl esters derived from fatty acids revealed that EstDZ2 can hydrolyze short- to medium-chain lengths fatty acid esters [15]. For esters with long chains, hydrolysis was barely detected. Optimal catalytic efficiency was detected for *p*-nitrophenyl butyrate [15].

Based on all these previous results, first we performed *in silico* analyses to provide insights of substrate structural features that influence enzyme activity and selectivity. Docking experiments performed for *p*-nitrophenyl butyrate and *p*-nitrophenyl octanoate hydrolysis catalyzed by EstDZ2 agreed with the results from the activity studies. More specifically, our *in silico* analyses revealed that binding of the *p*-nitrophenyl butyrate is more favorable as the substrate fits perfectly in the active site of the enzyme, thus EstDZ2 exhibits higher activity. As shown in Fig. 1, *p*-nitrophenyl octanoate binds in a different manner. In this case, a large part of the substrate does not fit in the active site but it is oriented towards the solvent and, therefore, this conformation is not very catalytically productive. These results are in complete agreement with the activity studies and underline that the activity of EstDZ2 is largely determined by the geometry of the active site and the structure of the bulky substrate. To depict the active site in a similar way in both cases (Fig. 1a and b), the catalytic serine was set to be in the lower center and the histidine of the catalytic triad in the middle left of the figures.

With these results at hand, a series of aryl *p*-, *o*- or *m*-substituted esters of butyric acid was synthesized bearing electron donating or electron withdrawing groups. The aim was to understand the catalytic behavior of EstDZ2 by rationally studying two structural elements of the substrates; (a) the position of the substituent of the aromatic ring and (b) the electronic character of the ring. The substituents of the aromatic ring chosen were: -OMe, -NO_2, -Br, -F and -propyl. Esters of butyric acid were readily prepared using a method based on Steglich esterification, using dicyclohexylcarbodiimide (DCC) and catalytic amount of 4-dimethylaminopyridine (DMAP) in the presence of dry dichloromethane (DCM) [19]. All the esters were obtained with good yields (Fig. 2).

Subsequently, we proceeded to EstDZ2-catalyzed hydrolysis of the substrates of interest under the optimal reaction conditions, that allow monitoring the EstDZ2-selectivity depending on electronic and/or steric effects. The progress of the reaction was monitored at various time intervals (5, 10, 15, 30, 60 min) as well as at 3 h, 5 h and 24 h, by assessing the conversion of the ester to the corresponding alcohol. Conversion rate was determined by gas chromatography using nonpolar column after comparing the retention time of the enzymatic reaction's products with the elution time of the corresponding ester and the alcohol. Before conducting the screening with EstDZ2, we tested the stability of each substrate ester under the standard enzymatic reaction conditions without addition of the enzyme (25 mM Tris-HCl buffer, pH 8 with 0.05% Triton X-100, 5.49 μmol of substrate, 50 °C). All the substrates are soluble in aqueous buffered solution, under the reaction conditions and only a small amount of alcohol was detected for most of the tested esters after 1 h in the buffer solution (2–8%).

As presented in Table 1, among the bromo substituted esters (entries 6–8), the *o*-bromophenyl ester (entry 8) was hydrolyzed more efficiently than the para and meta isomers. Interestingly, a similar trend was observed for nitro substituted esters (entries 2–4), among which better catalytic activity was observed for *o*-nitrophenyl butyrate (entry 4). These results demonstrate that EstDZ2 activity depends significantly on steric effects which determine the substrate acceptance. Among esters bearing substituents with altered electronic properties in para position (entries 2, 5, 6, 9 and 10), enhanced specific activity was observed for esters with halogen substituents (e.g. Br, F) (entries 6 and 9). However, in the case of a strong electron-withdrawing or electron donating substituent such as nitro and methoxy groups correspondingly, (*p*-nitrophenyl- and *p*-methoxyphenyl butyrates, entries 2 and 5) led to similar moderately enhanced activity. This result indicates that EstDZ2-catalyzed hydrolysis is independent on electronic effects. It appears that steric effects outweigh electronic effects and thus, mainly determine substrate acceptance. The highest hydrolytic activity among all tested esters was observed in the case of the larger bromo substituent in substrate *o*-bromophenyl butyrate (entry 8). This observation also confirms the steric dependence of the reaction activity. Highly efficient hydrolysis for all tested esters was observed at 5 h (conversions 85- > 99%), after addition of 0.3 μM EstDZ2 to 8 μmol of substrate in 4 mL Tris-HCl buffer 25 mM, pH 8.0, 0.05% Triton X-100, at 50 °C.

In an effort to gain deeper insight into the activity or enantioselectivity profile of EstDZ2, we investigated the hydrolysis of esters of secondary alcohols as substrates bearing one stereogenic center. They were synthesized by acetylation of the corresponding alcohols with acetic anhydride (Ac_2O) in anhydrous ethyl acetate (Fig. 3) [19].

Rac-1-phenylethyl acetate **11** was used for the standard reaction. Before proceeding to EstDZ2-catalyzed hydrolysis of this ester, *in silico* analysis was performed to predict which enantiomer of the ester would react faster. As seen in Fig. 4, the two enantiomers of *rac*-**11** bind to the active site of the enzyme in a similar manner. The carboxyl group of both (*R*)-**11** and (*S*)-**11** faces towards the catalytic Ser141, while both enantiomers are stabilized via π-π stacking with Phe222. The only difference between these two conformations is that for (*R*)-**11**, distance between the catalytic Ser and the carbonyl group of the ester is smaller. This observation indicates that *R* conformation would be slightly more catalytically favorable than the *S*.

In a typical run, 20 μmol of the substrate *rac*-**11** were diluted in 4 mL of buffer solution (25 mM Tris-HCl pH 8.0 buffer with 0.05% Triton X-100). The resulting suspension was shaken at 50 °C after the addition of the enzyme. Samples were collected periodically and were analyzed by GC analysis. Various amounts of enzyme were tested and the highest activity and enantioselectivity was achieved for 50 μg of EstDZ2. These were considered to be the optimal reaction conditions for the stereoselective hydrolysis of esters of secondary alcohols. The absolute configuration of the produced alcohol was determined by GC analysis using a chiral column. Comparison of the retention time with the corresponding data for the commercially available optically active (*S*)-1-phenylethanol revealed that the *R/S* enantiomeric ratio of the produced phenylethanol was 77/23. This faster hydrolysis for the *R*-

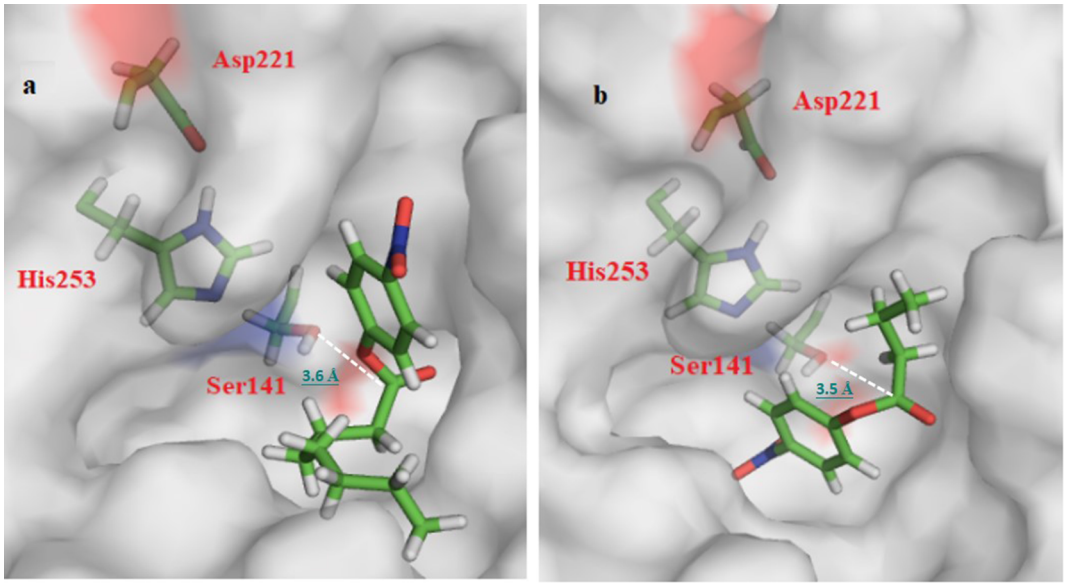

Fig. 1. Docking of *p*-nitrophenyl octanoate (a) and *p*-nitrophenyl butyrate (b) in the enzyme intermediate of EstDZ2. The catalytic residues are indicated in red. All figures were prepared with PYMOL 0.99. The distance from the catalytic Ser141 oxygen to the carbon atom in the carbonyl group is depicted with white dashed line. (For interpretation of the references to colour in this figure legend, the reader is referred to the web version of this article.)

enantiomer of *rac*-1-phenylethyl acetate **11** is in total agreement with the result from the docking studies performed for this substrate. This also provides extra evidence that the utilized *in silico* analysis can predict successfully the preferred enantiomer of substrates.

In addition to ester **11**, analogs with different alkyl, F or -OMe substituents in para position (esters 13–16) were investigated as well as the phenylethyl acetylate (ester **12**) for the enantioselective hydrolysis with EstDZ2. All substrates, including the model ester *rac*-**11** (entry 11) remained stable under the standard reaction conditions for 48 h in the absence of enzyme. The results obtained are summarized in Table 2.

According to the results shown in Table 2, activity and stereoselectivity of EstDZ2 is affected by steric hindrance factors. By increasing the substrate's chain length from methyl (entry 11) to ethyl (entry 12) there is a significant increase in the observed conversion at the same reaction time, but enantioselectivity decreases dramatically (conversion 17% and 25%, 54% *ee* and 10% *ee* respectively). In both cases EstDZ2 exhibits *R* enantioselectivity. It is interesting to note here that these preliminary results indicate that EstDZ2 follows the Kazlauskas rule, which predicts the enantiopreference of lipases towards hydrolysis of esters of secondary alcohols [21]. The enzyme activity was increased by increasing the size of the larger substituent (L) (entries 13–16). The same trend was observed in the enantioselectivity of the reaction (entries 13–15). The 1-(4-methoxyphenyl) ethyl acetate **16** was fully hydrolyzed in 24 h and no enantioselectivity was observed (conv. > 99%, < 1% *ee*).

3. Conclusions

A detailed activity and specificity analysis of the new thermostable carboxyl esterase EstDZ2 was performed in this work. EstDZ2 was found to be highly active in the hydrolysis of aryl-substituted esters of butyric acid bearing subtituents in the ortho position of the aromatic ring. While sole steric effects could be explained rationally, the impact of altered electronic properties did not follow a clear trend in all cases. These results indicate that substrate acceptance is mainly determined by steric effects.

Docking experiments revealed structural features of the enzyme that led to activity differences. By increasing the substrate's alkyl chain

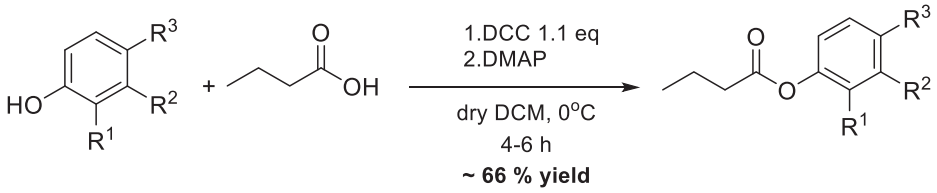

1: R^1 = H, R^2 = H, R^3 = H
2: R^1 = H, R^2 = H, R^3 = OMe
3: R^1 = NO_2, R^2 = H, R^3 = H
4: R^1 = H, R^2 = NO_2, R^3 = H
5: R^1 = H, R^2 = H, R^3 = NO_2
6: R^1 = H, R^2 = H, R^3 = $(CH_2)_2CH_3$
7: R^1 = H, R^2 = H, R^3 = F
8: R^1 = Br, R^2 = H, R^3 = H
9: R^1 = H, R^2 = Br, R^3 = H
10: R^1 = H, R^2 = H, R^3 = Br

Fig. 2. Esterification of substituted phenols with butyric acid.

Table 1
Substrate specificity for the enzymatic hydrolysis of aryl butyrate catalyzed by EstDZ2.

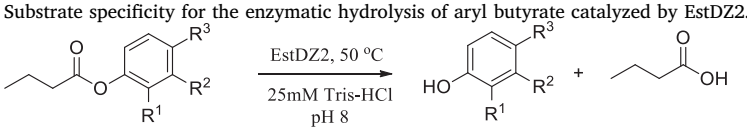

Entry	Substrate	Conversion[a] %				
		5 (min)	10 (min)	15 (min)	30 (min)	60 (min)
1	phenyl-butyrate	26	35	41	40	43
2	*p*-nitrophenyl butyrate	5	9	10	27	28
3	*m*-nitrophenyl butyrate	10	12	14	21	25
4	*o*-nitrophenyl butyrate	37	42	45	52	72
5	*p*-methoxyphenyl butyrate	8	13	10	13	35
6	*p*-bromophenyl butyrate	36	52	70	72	79
7	*m*-bromophenyl butyrate	34	58	67	75	71
8	*o*-bromophenyl butyrate	39	56	82	88	83
9	*p*-fluorophenyl butyrate	20	22	25	28	31
10	*p*-propylphenyl butyrate	9	17	14	29	56

[a] Conversions were derived from Gas Chromatography using nonpolar column and are in good agreement with the data obtained from ^{1}H NMR, (error ± 1%). Reaction conditions: 4 mL Tris-HCl buffer (25 mM, pH 8.0, 0.05% Triton X-100), substrate **1–10** (5.49 μmol), EstDZ2 (0.04 μM), 50 °C.

length from butyl to octyl, the activity of the enzyme decreased significantly since larger alkyl-groups do not appear to fit in the active site of the enzyme. EstDZ2 was also tested for the first time as a catalyst for the kinetic resolution of secondary alcohols. Preliminary studies revealed that this enzyme exhibits (*R*)-enantioselectivity. The bulkier the ester of secondary alcohol is, the higher activity and enantioselectivity was observed. The stereoselectivity of EstDZ2 was successfully predicted also by *in-silico* analysis. Further studies for the kinetic resolution of secondary alcohols are under investigation in our group.

4. Experimental section

4.1. General

NMR spectra were recorded on Bruker Avance series 500 and 300 spectrometers at room temperature. Chemical shifts (δ) are reported in ppm relative to the residual solvent peak ($CDCl_3$, δ: 7.26, $^{13}CDCl_3$, δ: 77.16) and the multiplicity of each signal is designated by the following abbreviations: s, singlet; d, doublet; t, triplet; q, quartet; m, multiplet; br, broad. Coupling constants (*J*) are quoted in Hz. Column chromatographic separations were carried out using a flash chromatography system with silica gel and hexane/ethyl acetate or petroleum ether/ethyl acetate solvent mixtures. Thin Layer Chromatography (TLC) was conducted using Merck silica gel (grade 60, F245). The progress of the enzymatic reactions was followed by gas chromatography using a SHIMADZU GC-2014 gas chromatograph equipped with an FID detector and non-polar column (HP-5 capillary, 30 m × 0.32 mm × 0.25 μm, 5% diphenyl and 95% dimethylpolysiloxane - Nonpolar). The progress of the EstDZ2-catalyzed hydrolysis of esters of secondary alcohols was followed by using a chiral column (J&W CP-Chirasil-Dex CB (25 × 0.25 × 0.25 μm) with total lengh 25 m).

4.2. Materials

Unless otherwise noted, all solvents and reagents were purchased from Sigma–Aldrich, Merck, Riedel or Fluka in the highest purity available and were used without any further purification. EstDZ2 was prepared as described previously by D. Zarafeta *et al.* [15].

4.3. General procedure for enzymatic hydrolysis of aryl substituted esters

The enzymatic hydrolysis was performed as follows: In a Tris-HCl buffer solution (4 mL, 25 mM, pH 8.0), the substrate (5.49 μmol) and the EstDZ2 (0.04 μM) were added. The reaction was incubated at 50 °C. Aliquots were withdrawn at predetermined time intervals and analyzed using GC. After completion of the reaction, the products were isolated by extracting the crude reaction mixture with EtOAc (3 × 1.5 mL). The combined organic layers were dried over $MgSO_4$ and evaporated to dryness.

4.4. General procedure for enzymatic hydrolysis of esters of secondary alcohols

In a vial of 22 mL, 4 mL of buffer solution Tris-HCl pH 8.0, 0.05% Triton-X 100 (v/v) were added. The reaction was incubated at 50 °C followed by the addition of 0.4 μM of EstDZ2 and 20 μmol of ester. After completion of the reaction, the products were isolated by extracting the crude reaction mixture with EtOAc (3 × 1.5 mL). The combined organic layers were dried over $MgSO_4$ and evaporated to dryness.

4.5. Steglich esterification

In a 50 mL round flask equipped with magnetic stirring, butyric acid (1 mmol), DCC (1.1 mmol) and DMAP (5%) were added with 10 mL of

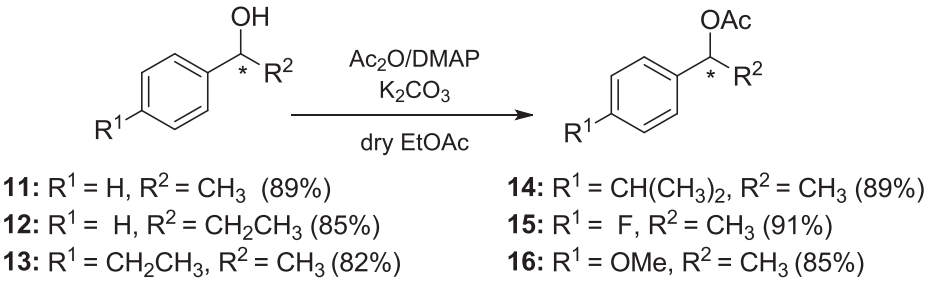

Fig. 3. Synthesis of acyl esters of secondary alcohols. The isolated yield is given in bracket.

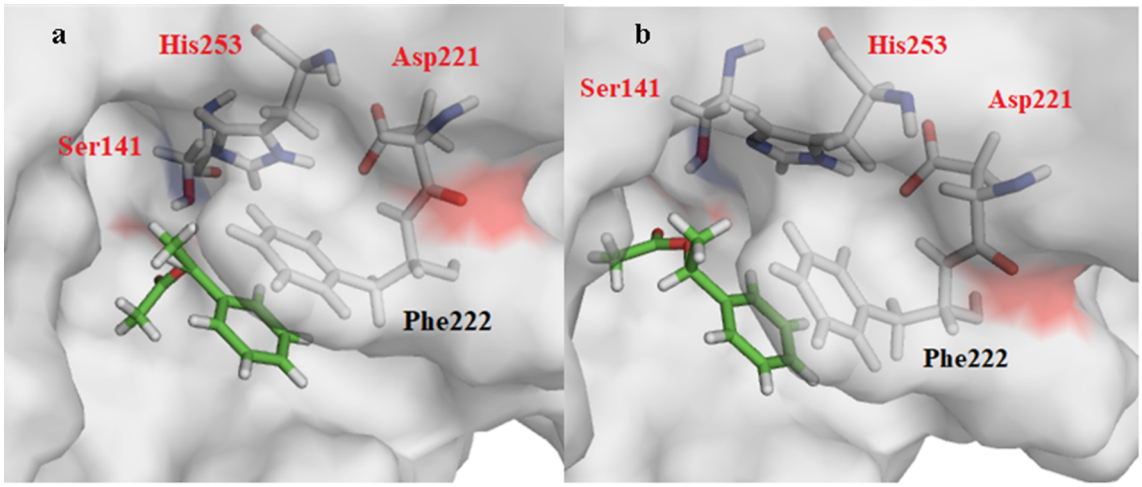

Fig. 4. Docking of (*R*)-1-phenylethyl acetate (green a) and (*S*)-1-phenylethyl acetate (green b) in the acetyl-enzyme intermediate of EstDZ2 active site. The catalytic residues are indicated in red. The distance between the oxygen of the hydroxyl group of the catalytic Ser141 and the carbonyl carbon of (*R*)- and (*S*)-phenyl ethyl acetate is 3.349 Å and 3.414 Å respectively. (For interpretation of the references to colour in this figure legend, the reader is referred to the web version of this article.)

Table 2
Kinetic resolution of esters of secondary alcohols using EstDZ2.

Entry	Substrate	Conversion[a] % (24 h)	Enantiomeric excess[b] %	E[c]
11		17	54	3.7
12		25	10	1.3
13	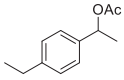	10	54	3.4
14	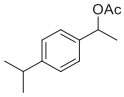	12	72	6.8
15	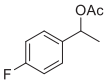	20	74	8.1
16	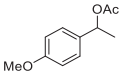	> 99	< 1	–

[a, b] Conversion and enantiomeric excess were derived from Gas Chromatography by using a chiral capillary column.
[c] E value was calculated as defined by Chen *et al.* [20].

dry CH_2Cl_2 at 0 °C. The mixture was kept under vigorous stirring for 30 min. Then, 3 mmol of alcohol dissolved in 4 mL of dry CH_2Cl_2 was added dropwise and the reaction was stirred for 6 h. After completion of the reaction the produced urea was filtered and the filtrate was evaporated. The product was purified by column chromatography with pet.ether/EtOAc (20:1) as eluent. Isolated yield of the pure corresponding ester ~ 66%.

*4.5.1. Phenyl butyrate **(1)***

Yield: 60%. ^{1}H NMR ($CDCl_3$ 500 MHz): δ 7.38 (t (dd), J = 8.4 Hz, 2H), 7.22 (t, J = 7.5 Hz, 1H), 7.08 (d, J = 7.8 Hz, 2H), 2.55 (t, J = 7.4 Hz, 2H), 1.84–1.76 (m, 2H), 1.05 (t, J = 7.4 Hz, 3H); ^{13}C NMR (500 MHz, $CDCl_3$): δ 172.3, 150.9, 129.5, 125.9, 121.7, 36.4, 18.6, 13.8.

*4.5.2. p-methoxyphenyl butyrate **(2)***

Yield: 65%. ^{1}H NMR ($CDCl_3$ 300 MHz): δ 7.00 (d, J = 9.12 Hz, 2H), 6.88 (d, J = 9.12 Hz, 2H), 3.79 (s, 3H), 2.52 (t, J = 7.32 Hz, 2H), 1.84–1.71 (m, 2H), 1.03 (t, J = 7.41 Hz, 3H); ^{13}C NMR (CDCl3, 500 MHz): δ 172.7, 157.3, 144.4, 122.5, 114.6, 55.7, 36.3, 18.6, 13.8.

*4.5.3. o-nitrophenyl butyrate **(3)***

Yield: 69%. ^{1}H NMR ($CDCl_3$ 500 MHz): δ 8.09 (dd, J_1 = 8.25 Hz, J_2 = 1.6 Hz, 1H), 7.65 (ddd, J_1 = 15.6 Hz, J_2 = 8.1 Hz, J_3 = 1.6 Hz, 1H), 7.39 (ddd, J_1 = 15.75 Hz, J_2 = 8.2 Hz, J_3 = 1.35 Hz, 1H), 7.23 (dd, J_1 = 8.1 Hz, J_2 = 1.25 Hz, 1H), 2.63 (t, J = 7.4 Hz, =2H), 1.85–1.77 (m, 2H), 1.06 (t, J = 7.4 Hz, 3H); ^{13}C NMR (CDCl3, 500 MHz): δ 171.2, 144.2, 141.9, 134.6, 126.5, 125.7, 125.2, 35.8, 18.0, 13.6.

*4.5.4. m-nitrophenyl Butyrate **(4)***

Yield: 64%. ^{1}H NMR ($CDCl_3$ 300 MHz): δ 8.11 (ddd, J_1 = 7.75 Hz, J_2 = 2.17 Hz, , J_3 = 1.00 Hz, 1H), 7.99 (t (dd), J_1 = 2.20 Hz, 1H), 7.56 (dd, J_1 = 8.20 Hz, 1H), 7.45 (ddd, J_1 = 8.15 Hz, J_2 = 2.25 Hz, J_3 = 1.00 Hz, 1H), 2.59 (t, J = 7.35 Hz, =2H), 1.84–1.77 (m, 2H), 1.06 (t, J = 7.35 Hz, 3H); ^{13}C NMR (CDCl3, 300 MHz): δ 171.6, 151.2, 148.9, 130.1, 128.3, 120.8, 117.5, 36.2, 18.4, 13.7.

*4.5.5. p-nitrophenyl butyrate **(5)***

Yield: 70%. ^{1}H NMR ($CDCl_3$ 300 MHz): δ 8.27 (d, J = 9.21 Hz, 2H), 7.28 (d, J = 9.27 Hz, 2H), 2.59 (t, J = 7.35 Hz, 2H), 1.84–1.76 (m, 2H), 1.05 (t, J = 7.38 Hz, 3H); ^{13}C NMR (CDCl3, 300 MHz): δ 171.3, 155.6, 145.5, 125.3, 122.6, 36.3, 18.4, 13.7.

*4.5.6. p-propylphenyl butyrate **(6)***

Yield: 64%. ^{1}H NMR ($CDCl_3$ 300 MHz): δ 7.16 (d, J = 8.45 Hz, 2H), 6.97 (d, J = 8.45 Hz, 2H), 2.57 (t, J = 7.50 Hz, 2H), 2.52 (t, J = 7.35 Hz, 2H), 1.82–1.74 (m, 2H), 1.66–1.59 (m, 2H), 1.04 (t, J = 7.40 Hz, 3H), 0.93 (t, J = 7.35 Hz, 3H); ^{13}C NMR (CDCl3, 300 MHz): δ 172.5, 148.8, 140.3, 129.4, 121.3, 37.6, 36.4, 24.7, 18.6, 13.9, 13.8.

*4.5.7. p-fluorophenyl butyrate **(7)***

Yield: 69%. ^{1}H NMR ($CDCl_3$ 300 MHz): δ 7.07–7.04 (m, 4H), 2.53 (t, J = 7.35 Hz, 2H), 1.82–1.74 (m, 2H), 1.04 (t, J = 7.40 Hz, 3H); ^{13}C NMR (CDCl3, 500 MHz): δ 172.3, 161.3, 159.3, 146.70, 146.68, 123.13, 123.06, 116.2, 116.1, 36.3, 18.6, 13.8.

*4.5.8. o-bromophenyl butyrate **(8)***

Yield: 68%. ^{1}H NMR ($CDCl_3$ 300 MHz): δ 7.60 (dd, J_1 = 8.31 Hz,

J_2 = 1.71 Hz, 1H), 7.35–7.30 (m, 1H), 7.20–7.09 (m, 2H), 2.60 (t, J = 7.32 Hz, 2H), 1.89–1.77 (m, 2H), 1.07 (t, J = 7.38 Hz, 3H); ^{13}C NMR (CDCl3, 300 MHz): δ 171.4, 148.4, 133.5, 128.6, 127.4, 124.0, 116.4, 36.1, 18.5, 13.9.

4.5.9. m-bromophenyl Butyrate (9)

Yield: 63%. ^{1}H NMR ($CDCl_3$ 300 MHz): δ 7.36 (ddd, J_1 = 8.05 Hz, J_2 = 1.8 Hz, , J_3 = 0.95 Hz, 1H), 7.28 (t , J_1 = 2.05 Hz, 1H), 7.24 (t, J_1 = 8.15 Hz, 1H), 7.04 (ddd, J_1 = 8.15 Hz, J_2 = 2.20 Hz, J_3 = 0.95 Hz, 1H), 2.53 (t, J = 7.50 Hz, =2H), 1.82–1.74 (m, 2H), 1.04 (t, J = 7.35 Hz, 3H); ^{13}C NMR (CDCl3, 500 MHz): δ 171.8, 151.4, 130.6, 129.0, 125.3, 122.5, 120.6, 36.3, 18.5, 13.8.

4.5.10. p-bromophenyl butyrate (10)

Yield: 63%. ^{1}H NMR ($CDCl_3$ 300 MHz): δ 7.48 (d, J = 8.79 Hz, 2H), 6.97 (d, J = 8.73 Hz, 2H), 2.50 (t, J = 7.35 Hz, 2H), 1.83–1.71 (m, 2H), 1.03 (t, J = 7.41 Hz, 3H), ^{13}C NMR (CDCl3, 500 MHz): δ 171.9, 149.9, 132.6, 123.5, 118.9, 36.3, 18.5, 13.8.

4.6. Acetylation of secondary alcohols

In a 100 mL round flask equipped with magnetic stirring, the secondary alcohol (1 mmol) was added with 7 mL of EtOAc. Next, acetic anhydride (2 mmol), K_2CO_3 (4 mmol) and catalytic amount of DMAP (5%) were added and the mixture was stirred at room temperature for the appropriate time (24 h, monitored by TLC). After completion, the reactant was filtered and water was added to the filtrate. The mixture was extracted with ethyl acetate (10 mL × 3) and the combined organic layer was washed with saturated $NaHCO_3$ (10 mL × 2), brine (10 mL), driedover MgSO4 and concentrated to give the pure product. Isolated yield ~ 87%.

4.6.1. 1-phenylethyl acetate (11)

Yield: 89%. ^{1}H NMR ($CDCl_3$ 500 MHz): δ 7.36–7.27 (m, 5H), 5.88 (q, J = 6.6 Hz, 1H), 2.07 (s, 3H), 1.52 (d, J = 6.6 Hz, 3H); ^{13}C NMR (500 MHz, $CDCl_3$): δ 170.5, 141.8, 128.6, 128.0, 126.2, 72.5, 22.3, 21.5.

4.6.2. 1-phenylpropyl acetate (12)

Yield: 85%. ^{1}H NMR ($CDCl_3$ 500 MHz): δ 7.36–7.27 (m, 5H), 5.66 (t, J = 7.3 Hz, 1H), 2.08 (s, 3H), 1.99–1.88 (m, 1H), 1.86–1.77 (m, 1H), 0.88 (t, J = 7.4 Hz, 3H); ^{13}C NMR (500 MHz, $CDCl_3$): δ 170.6, 140.7, 128.5, 128.0, 126.7, 77.5, 29.4, 21.4, 10.1.

4.6.3. 1-(4-ethylphenyl)ethyl acetate (13)

Yield: 82%. ^{1}H NMR ($CDCl_3$ 500 MHz): δ 7.28 (d, J = 8.05 Hz, 2H), 7.18 (d, J = 8.25 Hz, 2H), 5.87 (q, J = 6.6 Hz, 1H), 2.64 (q, J = 7.35 Hz, 2H), 2.06 (s, 3H), 1.53 (d, J = 6.6 Hz, 3H), 1.23 (t, J = 7.6 Hz, 3H); ^{13}C NMR (300 MHz, $CDCl_3$): δ 170.6, 144.1, 139.0, 128.1, 126.3, 72.4, 28.7, 22.2, 21.6, 15.7.

4.6.4. 1-(4-isopropylphenyl)ethyl acetate (14)

Yield: 89%. ^{1}H NMR ($CDCl_3$ 500 MHz): δ 7.28 (d, J = 8.15 Hz, 2H), 7.21 (d, J = 8.10 Hz, 2H), 5.87 (q, J = 6.6 Hz, 1H), 2.94–2.86 (m, 1H), 2.06 (s, 3H), 1.53 (d, J = 6.6 Hz, 3H), 1.24 (d, J = 6.95 Hz, 6H); ^{13}C NMR (500 MHz, $CDCl_3$): δ 170.4, 148.5, 138.9, 126.5, 126.1, 72.2, 33.8, 23.9, 22.0, 21.4.

4.6.5. 1-(4-fluorophenyl)ethyl acetate (15)

Yield: 91%. ^{1}H NMR ($CDCl_3$ 500 MHz): δ 7.3.4–7.31 (m, 2H), 7.05–7.01 (m, 2H), 5.85 (q, J = 6.6 Hz, 1H), 2.06 (s, 3H), 1.52 (d, J = 6.6 Hz, 3H) ; ^{13}C NMR (500 MHz, $CDCl_3$): δ 170.2, 163.3, 161.3, 137.5, 137.4, 127.9, 127.8, 115.4, 115.2, 71.6, 22.1, 21.3.

4.6.6. 1-(4-methoxyphenyl)ethyl acetate (16)

Yield: 85%. ^{1}H NMR ($CDCl_3$ 500 MHz): δ 7.29 (d, J = 8.60 Hz, 2H), 6.88 (d, J = 8.65 Hz, 2H), 5.85 (q, J = 6.6 Hz, 1H), 3.80 (s, 3H), 2.05 (s, 3H), 1.52 (d, J = 6.6 Hz, 3H); ^{13}C NMR (500 MHz, $CDCl_3$): δ 170.3, 159.2, 133.7, 127.6, 113.8, 72.0, 55.2, 21.9, 21.4.

4.7. In silico analysis

In silico analyses were performed using the YASARA 18.11.21 software. All esters used as substrates were drawn in YASARA and refined under the AMPER03 force field. The docking experiments were performed in a water cell (pH 8.0, 50 °C). The protein ("receptor") was flexible during docking simulations. Four parameters were used to identify productive clusters from analysis of the substrate–protein complexes: 1) protein distortion, 2) stability of the hydrogen bond interactions with the oxyanion hole residues, 3) localization of the hydroxyl group with regard to the region included between the catalytic histidine and serine residues, and 4) a distance of less than 4 Å between the catalytic serine and the substrate. All figures were prepared with PyMOL 0.99.

Declaration of Competing Interest

The authors declare that they have no known competing financial interests or personal relationships that could have appeared to influence the work reported in this paper.

Appendix A. Supplementary data

Supplementary data to this article can be found online at https://doi.org/10.1016/j.bioorg.2020.104214.

References

[1] M. Levisson, J. Van der Oost, S.W.M. Kengen, Carboxylic ester hydrolases from hyperthermophiles, Extremophiles 13 (2009) 567, https://doi.org/10.1007/s00792-009-0260-4.

[2] M. Fischer, J. Pleiss, The Lipase Engineering Database: a navigation and analysis tool for protein families, Nucleic Acids Res. 31 (1) (2003) 319–321, https://doi.org/10.1093/nar/gkg015.

[3] R. Verger, 'Interfacial activation' of lipases: facts and artifacts, Trends Biotechn. 15 (1997) 32–38, https://doi.org/10.1016/S0167-7799(96)10064-0.

[4] A. Hjorth, F. Carrière, C. Cudrey, H. Woldike, E. Boel, D.M. Lawson, F. Ferrato, C. Cambillau, G.G. Dodson, L. Thim, R. Verger, A structural domain (the lid) found in pancreatic lipases is absent in the guinea pig (phospho) lipase, Biochemistry 32 (1993) 4702–4707, https://doi.org/10.1021/bi00069a003.

[5] H.W. Anthonsen, A. Baptista, F. Drabløs, P. Martel, S.B. Petersen, M. Sebastião, L. Vaz, Lipases and esterases: a review of their sequences, structure and evolution, Biotechnol. Annu. Rev. 1 (1995) 315–371, https://doi.org/10.1016/S1387-2656(08)70056-5.

[6] P.C. Kienesberger, M. Oberer, A. Lass, R. Zechner, Mammalian patatin domain containing proteins: a family with diverse lipolytic activities involved in multiple biological functions, J. Lipid Res. 50 (2008) 63–68, https://doi.org/10.1194/jlr.R800082-JLR200.

[7] M.S. Jensen, S.K. Jensen, K. Jakobsen, Development of digestive enzymes in pigs with emphasis on lipolytic activity in the stomach and pancreas, J. Anim. Sci. 75 (2) (1997) 437, https://doi.org/10.2527/1997.752437x.

[8] a) S. Sharma, S.S. Kanwar, Organic solvent tolerant lipases and applications, Sci. World J. 625258 (2014), https://doi.org/10.1155/2014/625258;
b) K.R. Jegannathan, P.H. Nielsen, Environmental assessment of enzyme use in industrial production – a literature review, J. Cleaner Prod. 42 (2013) 228–240, https://doi.org/10.1016/j.jclepro.2012.11.005.

[9] A.M. Klibanov, Improving enzymes by using them in organic solvents, Nature 409 (2001) 241–246, https://doi.org/10.1038/35051719.

[10] N. Gurung, S. Ray, S. Bose, V. Rai, A broader view: microbial enzymes and their relevance in industries, medicine, and beyond, BioMed Res. Int. 2013 (2013) 1–18, https://doi.org/10.1155/2013/329121.

[11] J.L. Adrio, A.L. Demain, Microbial enzymes: tools for biotechnological processes, Biomolecules 4 (2014) 117–139, https://doi.org/10.3390/biom4010117.

[12] P. Hugenholtz, G.W. Tyson, Metagenomics, Nature 455 (7212) (2008) 481–483, https://doi.org/10.1038/455481a.

[13] P. Menzel, R. Gudbergsd, G. Rike, L. Lin, Q. Zhang, P. Contursi, M. Moracci, J.K. Kristjansson, B. Bolduc, S. Gavrilov, N. Ravin, A. Mardanov, E. Bonch-Osmolovskaya, M. Young, A. Krogh, X. Peng, Comparative metagenomics of eight geographically remote terrestrial hot springs, Microb. Ecol. 70 (2) (2015) 411–424, https://doi.org/10.1007/s00248-015-0576-9.

[14] R. Wohlgemuth, J. Littlechild, D. Monti, K. Schnorr, B. Siebers, P. Menzel, T. van Rossum, I. Kublanov, A.G. Rike, G. Skretas, Z. Szabo, X. Peng, M.J. Young,

Discovering of novel hydrolases from hot environments, Biotechnol. Adv. 36 (8) (2018) 2077–2100, https://doi.org/10.1016/j.biotechadv.2018.09.004.
[15] D. Zarafeta, D. Moschidi, E. Ladoukakis, S. Gavrilov, E.D. Chrysina, A. Chatziioannou, I. Kublanov, G. Skretas, F.N. Kolisis, Metagenomic mining for thermostable esterolytic enzymes uncovers a new family of bacterial esterases, Sci. Rep. 6 (1) (2016), https://doi.org/10.1038/srep38886.
[16] L.E. Janes, A.C. Löwendahl, R.J. Kazlauskas, Quantitative screening of hydrolase libraries using ph indicators: identifying active and enantioselective hydrolases, Chem. Eur. J. 4 (11) (1998) 2324–2331, https://doi.org/10.1002/(SICI)1521-3765(19981102)4:11<2324::AID-CHEM2324>3.0.CO;2-I.
[17] A.M.F. Liu, N.A. Somers, R.J. Kazlauskas, T.S. Brush, F. Zocher, M.M. Enzelberger, U.T. Bornscheuer, G.P. Horsman, A. Mezzeti, C. Schmidt-Dannert, R.D. Schmid, Mapping the substrate selectivity of new hydrolases using colorimetric screening: lipases from Bacillus thermocatenulatus and Ophiostoma piliferum, esterases from Pseudomonas fluorescens and Streptomyces diastatochromogenes, Tetrahedron: Asymmetry 12 (4) (2001) 545–556, https://doi.org/10.1016/S0957-4166(01)00072-6.
[18] J. Pliego, J. Mateos, J. Rodriguez, F. Valero, M. Baeza, R. Femat, E. Herrera- López, Monitoring lipase/esterase activity by stopped flow in a sequential injection analysis system using p-nitrophenyl butyrate, Sensors 15 (2) (2015) 2798–2811, https://doi.org/10.3390/s150202798.
[19] W. Steglich, B. Neises, Simple method for the esterification of carboxylic acids, Angew. Chem. Int. Ed. Engl. 7 (1978) 17, https://doi.org/10.1002/anie.197805221.
[20] C.S. Chen, Y. Fujimoto, G. Girdaukas, C.J. Sih, Quantitative analyses of biochemical kinetic resolutions of enantiomers, J. Am. Chem. Soc. 104 (1982) 7294–7299, https://doi.org/10.1021/ja00389a064.
[21] R.J. Kazlauskas, A.N.E. Weissfloch, A.T. Rappaport, L.A. Cuccia, A rule to predict which enantiomer of a secondary alcohol reacts faster in reactions catalyzed by cholesterol esterase, lipase from Pseudomonas cepacia, and lipase from Candida rugosa, J. Org. Chem. 56 (8) (1991) 2656–2665, https://doi.org/10.1021/jo00008a016.